Published in final edited form as:
J Magn Reson Imaging. 2013 July ; 38(1): 36–45. doi:10.1002/jmri.23961.

Complexity and Synchronicity of Resting State BOLD FMRI in Normal Aging and Cognitive Decline

Collin Y Liu, MD[1,2,3,4], **Anitha P Krishnan, PhD**[3], **Lirong Yan, PhD**[1], **Robert X Smith, PhD**[1], **Emily Kilroy, MS**[1], **Jeffery R Alger, PhD**[1], **John M Ringman, MD**[1,5], and **Danny JJ Wang, PhD, MSCE**[1,*]

[1]Department of Neurology, University of California Los Angeles, Los Angeles, CA 90095, USA

[2]Neurobehavior Unit, Greater Los Angeles Veterans Administration Healthcare System, Los Angeles, CA 90073, USA

[3]Department of Neurology, University of Southern California, Los Angeles, CA 90033, USA

[4]Department of Radiology, University of Southern California, Los Angeles, CA 90033, USA

[5]Mary S. Easton Center for Alzheimer's Disease Research, University of California Los Angeles, Los Angeles, CA 90095, USA

Abstract

Purpose—To explore the use of approximate entropy (ApEn) as an index of the complexity and the synchronicity of resting state BOLD fMRI in normal aging and cognitive decline associated with familial Alzheimer's disease (fAD).

Materials and Methods—Resting state BOLD fMRI data were acquired at 3T from 2 independent cohorts of subjects consisting of healthy young (age 23±2 years, n=8) and aged volunteers (age 66±3 years, n=8), as well as 22 fAD associated subjects (14 mutation carriers, age 41.2±15.8 years; and 8 non-mutation carrying family members, age 28.8±5.9 years). Mean ApEn values were compared between the two age groups, and correlated with cognitive performance in the fAD group. Cross-ApEn (C-ApEn) was further calculated to assess the asynchrony between precuneus and the rest of the brain.

Results—Complexity of brain activity measured by mean ApEn in gray and white matter decreased with normal aging. In the fAD group, cognitive impairment was associated with decreased mean ApEn in gray matter as well as decreased regional ApEn in right precuneus, right lateral parietal regions, left precentral gyrus, and right paracentral gyrus. A pattern of asynchrony between BOLD fMRI series emerged from C-ApEn analysis, with significant regional anti-correlation with cross-correlation coefficient of functional connectivity analysis.

Conclusion—ApEn and C-ApEn may be useful for assessing the complexity and synchronicity of brain activity in normal aging and cognitive decline associated with neurodegenerative diseases

Keywords

Resting state BOLD fMRI; Approximate Entropy (ApEn); Complexity; Aging; Familial Alzheimer's disease (fAD); Default mode network (DMN)

[*]**Corresponding Author:** Danny JJ Wang, PhD, MSCE, Department of Neurology, University of California Los Angeles, 660 Charles E Young Dr South, Los Angeles, CA 90095, USA, jwang71@gmail.com, 310-983-3667 (phone) 310-794-7406 (fax).

INTRODUCTION

Complexity is one of the key features defining the behavior of physiological systems of a living organism (1). This complexity arises from the interaction of an array of interconnected physiological systems and regulatory feedback loops, enabling the organism to adapt to the stresses of everyday life. Continuous interplay among multiple components of these systems at molecular, cellular, organ, and systemic levels ensures that information is constantly exchanged, even as the organism rests. It is therefore important to measure and characterize the complex temporal dynamics of physiological systems over time, not captured by statistical measures such as the mean or standard deviation (SD), as a means to improve the diagnosis and treatment of human diseases.

During the past few decades, a variety of measures derived from the fields of nonlinear statistics and information theory have been developed to describe the dynamics of physiological systems (2). Many of these are based on the concept of fractals (3). Fractal processes are characterized by "self-resemblance" over multiple measurement scales, and their frequency spectra typically show an inverse power-law ($1/f$-like) scaling pattern (4). The mean rate of creation of information, also known as the Kolmogorov-Sinai (KS) entropy, is a useful parameter to characterize the system dynamics (5). The KS entropy for “real-world” time series of finite length, however, cannot usually be estimated with reasonable precision. For the analysis of such typically short, noisy time series, Pincus introduced approximate entropy (ApEn) as a family of non-linear statistics to quantify regularity in serial data (6). Higher ApEn values generally implicate that the process is less predictable (or more complex). ApEn and its variants have been successfully applied to biological signals such as cardiac electric activity (ECG), heart rate, blood pressure, respiratory patterns, brain electric activity (EEG), mood ratings, and hormonal release, to distinguish healthy function from disease, and to predict the onset of adverse health-related events (7–12). A general trend of decreasing complexity of physiological signals with aging has also been reported (1).

Among human organs, the brain is the most complex information processing system with 10–100 billion neurons and 10^{14} synapses. Functional MRI based on the blood-oxygen-level-dependent (BOLD) contrast is one of the most widely used methods for noninvasively monitoring the temporal dynamics of brain physiology (e.g. cerebral blood flow) and neuronal activity. Resting state BOLD fMRI time-series may possess fractal properties, since its power spectrum is well characterized by the $1/f$ function (13–15). There has been converging evidence suggesting that temporal fluctuations in resting state BOLD fMRI, in particular low frequency components (<0.1Hz), arise primarily from spontaneous fluctuations of brain physiology and neuronal activity (16,17). To date, the analysis of resting-state BOLD fMRI has been limited to conventional linear statistics such as cross-correlation and amplitude of low frequency fluctuations (18,19). Only one study has used ApEn to analyze BOLD fMRI time-series acquired when subjects were performing a visual information processing task (20). Higher ApEn was found to be associated with better cognitive performance in 40 individuals aged 68 to 70. One limitation of this study is the potential confounding effect of block design and task performance on the ApEn measure of fMRI series. The primary goal of the present study is to explore the use of ApEn as a measure of regularity or complexity of resting-state BOLD fMRI in two independent cohorts of subjects consisting of healthy young and aged volunteers as well as symptomatic and presymptomatic persons carrying familial Alzheimer’s disease (fAD) mutations. Our hypothesis is that ApEn decreases with normal aging as well as in fAD subjects with deteriorating cognitive/behavioral performance.

In addition to ApEn, which assesses the complexity of individual time-series, the asynchrony between two time-series can be characterized by cross-approximate entropy (C-ApEn)(6). C-ApEn measures the relative pattern orderliness of two time series, with lower C-ApEn values denoting greater conditional regularity or synchronicity. While C-ApEn may be intuitively understood as the opposite of temporal correlation that forms the basis of resting-state functional connectivity, temporal correlation analyses assume that resting-state BOLD fMRI series is a temporally stationary process. Evidence from both task-based fMRI studies and animal electrophysiology suggests that functional connectivity may exhibit dynamic changes within time scales of seconds to minutes (21). Therefore, non-linear statistics such as C-ApEn may provide alternative and complementary measures to temporal correlation analysis of functional connectivity. The second aim of the present study is to apply C-ApEn to resting state BOLD fMRI to quantify the asynchrony of each voxel relative to a reference or seed voxel. We hypothesize that the pattern of asynchrony between BOLD fMRI time-series by C-ApEn analysis will show regional anti-correlation with cross-correlation coefficient, a key measure of functional connectivity analyses.

MATERIALS AND METHODS

Subjects

Two experiments (Exp 1 and 2) were performed to investigate the effect of healthy aging and cognitive decline associated with fAD on ApEn of resting-state BOLD fMRI, respectively. For Exp 1, a total of 16 healthy subjects, 8 young (age 23±2 yrs, 6 males) and 8 elderly subjects (age 66±3 yrs, 5 males), participated after they provided written informed consent. All participants were screened for neurological or psychiatric illnesses. For Exp 2, 22 subjects with pathogenic autosomal dominant mutations participated after they or their legal representative provided written informed consent. Fourteen of the 22 subjects, 9 females and 5 males, with age 41.2±15.8 yrs, were mutation carriers. Twelve of the 14 mutation carriers had presenilin-1 (PSEN1) mutations and two had an amyloid precursor protein (APP) mutation. Of the 14 mutation carriers, 4 were asymptomatic (Clinical Dementia Rating/CDR = 0), 7 had mild cognitive impairment (CDR = 0.5) and 3 were demented (one with a CDR score of 1, and 2 with CDR scores of 3). Eight of the 22 subjects were non-mutation carrying family members, with 5 females and 3 males, and age 28.8±5.9 yrs. Subjects were participants in a comprehensive multicenter clinical, imaging, and biochemical marker study to evaluate early changes occurring in persons carrying fAD mutations (the Dominantly Inherited Alzheimer Network, NIH U01-AG032438). Subjects underwent Mini Mental Status Exam (MMSE) and Clinical Dementia Rating (CDR) tests (22, 23). All clinical evaluations were performed blind to participant's genetic status.

Data Acquisition

All MRI experiments were performed on Siemens Tim Trio 3T scanners (Erlangen, Germany) using 12-channel head coil. In Exp 1, subjects underwent a resting-state BOLD fMRI scan with their eyes open. A single-shot dual-echo gradient-echo echo-planar imaging (EPI) sequence with interleaved TE was used to acquire 4 different TE data sets for every 2 consecutive TRs (TE1=20ms and TE2=50ms for one TR, TE3=35ms and TE4=65ms for the following TR)(24). The purpose of this multi-echo EPI sequence was to account for potential changes of T2* between the two age groups, as well as to investigate the effect of TE on ApEn. Each scan with 240 acquisitions took 8 min. Ten oblique slices with 5mm thickness and 1mm gap were scanned parallel to the anterior-posterior commissure (AC-PC). Other parameters included: FOV=22cm; matrix=64 × 64; TR=1000ms (effective TR = 2000ms); flip angle=65°. In Exp 2, resting-state BOLD fMRI scans were performed on subjects with their eyes open. Gradient-echo EPI sequence was performed with the following imaging parameters: TR/TE=2000/35ms, FOV=22cm, matrix=64×64, 35 slices

with thickness of 4mm, 140 acquisitions with a scan time of 4.7min. In both Exp 1 and 2, conventional T1 weighted 3D images were acquired using an MPRAGE sequence (TR/TE/TI=1730/3.96/1100ms; flip angle=15°; matrix=256 × 256×192, voxel size=1 × 1 × 1 mm^3) for anatomic MRI.

Data Processing

The fMRI data were realigned to correct for motion using SPM 8 (Wellcome Department of Cognitive Neurology, UCL, UK), followed by co-registration with T1-weighted structural MRI. Whole-brain, gray matter, white matter, and cerebrospinal fluid (CSF) masks were segmented based on T1-weighted structural MRI. Whole brain ApEn and C-ApEn were calculated voxel by voxel using a custom Matlab program, as described below. Average ApEn values of gray matter, white matter, and CSF were calculated using the corresponding masks in each subject. For regional analyses, ApEn and C-ApEn volumes were normalized to the MNI space.

Calculation of ApEn

As described in the 1991 paper by Pincus (6), the calculation of ApEn depends on 2 parameters: m and r. ApEn measures the logarithmic likelihood (or conditional probability) that runs of patterns that are close (within the same tolerance width r) for m contiguous observations remain close on subsequent incremental comparisons ($m+1$). The steps involved in calculating ApEn are as follows:

1. For a time-series u(t) with N data points, form sequence of vectors x(1), x(2), …,x(N) by x(i) = [u(i),…,u(i+m-1)].
2. For each i, 1≤ i ≤ N-m+1, construct $C_i^m(r)$ = {number of x(j) such that d[x(i),x(j)] ≤ r }/ (N+m-1), where d[x(i),x(j)] = max|u(i+k-1)-u(j+k-1)| for k = 1,2,...,m, given by the maximum of the difference of the scalar components of x(i) and x(j), represents the distance between the vectors.
3. Calculate $C_m(r)=\frac{\sum_{j=1}^{N-m+1} C_i^m(r)^j}{N-m+1}$.
4. Repeat steps 1, 2 and 3 for m+1 contiguous observations to obtain $C_{m+1}(r)$.
5. ApEn is defined as: ApEn(m, r, N) = ln $C_m(r)$ - ln $C_{m+1}(r)$.

The parameters used for calculating ApEn were: m=1 to 5 and r=0.25 × standard deviation (SD) of the fMRI time series. In Exp 1, we calculated ApEn values for m=1 to 5 to empirically understand ApEn variations with m. According to Richman *et al* (25), reasonable estimates of these conditional probabilities are achieved with an N value of at least 10^m and preferably at least 30^m points. Based on the above observation, and with N=240 or 140 in our experiments, the ApEn values were acceptable only for m = 1 and 2.

Calculation of C-ApEn

The calculation of C-ApEn was identical to that of ApEn except two different time series were compared. A reference voxel (2 mm-radius sphere) in the left precuneus was visually selected by a neurologist (CYL) to match the peak coordinate (x=−6, y=−58, z=28) of the default mode network (DMN) based on a meta-analysis (26). C-ApEn values were calculated for all the voxels in the brain against the time-series of the reference voxel. For each calculation, the two time-series were normalized to have zero-mean and the same range of SD. Self-comparisons were eliminated to avoid bias from self-matching. However, C-ApEn is not defined when the two time-series have no matching sub-series (i.e. m or m+1

contiguous observations). In our algorithm, we assigned C-ApEn = 0 when there were no matching sub-series. For comparison, conventional cross-correlation analysis was performed using the same seed voxel as in C-ApEn analysis, using the REST software (27). C-ApEn and cross-correlation coefficients were then correlated voxel by voxel.

Statistical Analyses

Statistical analyses were performed using the SPSS 16.0 software (SPSS, Inc., Chicago, IL, USA). Mean ApEn values in gray and white matter and also between the old and young groups were compared using multivariate ANOVA with age group as the between-subject factor, TE and tissue type as within subject factors. Spearman correlation coefficients were used to assess correlations between mean ApEn values and cognitive performance in fAD subjects. Corresponding voxel-wise analyses were carried out in SPM 8. For Exp 1, normalized ApEn maps were compared between young and aged subjects using general linear model (GLM) with a factorial design (age group and TE) to include data from 4 TEs, as well as using unpaired t-test for each TE respectively. For Exp 2, GLM analysis was carried out to investigate associations between ApEn and cognitive/behavioral performances indicated by MMSE and CDR Sum of Box (SOB) scores, with age and mutation status included as covariates. Significant activations were first detected with the threshold of uncorrected $p<0.001$ and a cluster size of at least 10 voxels. Small volume correction was further performed on detected activation clusters, using the region-of-interest (ROI) masks provided by Automated Anatomical Labeling toolbox (http://www.fil.ion.ucl.ac.uk/spm/ext/#AAL). In addition, mean ApEn values were correlated with the maximum translation displacement and rotation angle of 6 rigid-body motion parameters across 22 subjects in Exp 2 to investigate the potential confounding effect of head motion on ApEn values.

RESULTS

Empirical Analysis of Parameters m and r

The sliding window width (m) was varied from 1 to 5 using BOLD fMRI data acquired in Exp 1. As shown in Fig. 1 of 2 representative subjects, ApEn is highest at m=1, and it decreases toward 0 as m increases. This trend was highly consistent across all young and aged subjects. The effect of tolerance width (r) on ApEn was also evaluated, which is defined as a percentage of the SD of the time-series. As shown in Fig. 2, ApEn is highest when r is around 25–30% of SD, which is consistent with a recent study on task-evoked BOLD fMRI (20). These empirical observations, in conjunction with the suggested m and r values in literature (6,10), justify our choosing m=2 for the calculation of ApEn with r=0.25 × SD in all of the following analyses.

Effects of Echo Time and Tissue Type

Figure 3 shows the mean ApEn values acquired at the 4 TEs (20, 35, 50, 65ms) in the 2 age groups in 3 tissue types respectively. Multivariate ANOVA showed that there was a significant main effect of TE on mean ApEn values in gray matter ($F(3, 12)=9.657$, $p=0.002$), white matter ($F(3, 12)=46.83$, $p<0.001$), and CSF ($F(3, 12)=318.8$, $p<0.001$). In all the tissue types, lowest ApEn values were observed at the TE of 35ms, which was verified by post hoc pairwise comparison of ApEn values acquired at 4 TEs ($p<0.05$). Nevertheless, the fitted mean T2* values were not different between the young (T2* = 51.21±2.63ms) and aged (T2* = 51.19±2.70ms) subjects.

Multivariate ANOVA also showed that there was a significant main effect of tissue type on mean ApEn values in the 2 age groups across 4 TEs ($F(2, 13) \geq 12.12$, $p \leq 0.001$)(see Fig. 3). Post hoc analyses showed that mean ApEn values in white matter were significantly

greater than those of CSF ($p<0.02$). Mean ApEn values in white matter were also greater than those of gray matter ($p<0.05$) at the TE of 20, 35 and 50ms.

ApEn Changes in Normal Aging

Multivariate ANOVA showed that there was a significant main effect of age on mean ApEn values in gray matter ($F(1, 14)=36.72$, $p<0.001$) and white matter ($F(1, 14)=14.72$, $p=0.002$), but not in CSF ($F(1, 14)=1.99$, $p=0.18$). As shown in Fig. 4 of the representative ApEn maps acquired at the TE of 35ms, mean ApEn in gray matter of the young group (1.10±0.005) was significantly higher than that of the aged group (1.07±0.016, $p<0.001$). In white matter, mean ApEn of the young group (1.14±0.015) was also significantly higher than that of the old group (1.09±0.026, $p=0.002$). As expected, ApEn of CSF did not show significant difference between the 2 age groups ($p=0.34$). Voxel-wise comparison of ApEn between young and aged groups, using GLM with a flexible factorial design to include all 4 TEs, revealed no significant clusters. However, two-sample t-test analysis of the young and aged groups at each TE showed significantly decreased regional ApEn in aged subjects. No increased regional ApEn with age was found. For the representative TE of 35ms, significantly decreased ApEn was found in bilateral angular gyri (AG), right mid temporal gyrus (MTG), left supramarginal gyrus (SMG), left mid and posterior cingulate (MC and PC), and left calcarine cortex (Cal) at the threshold of $p=0.001$ (uncorrected) and a minimum cluster size (kc) of 10 voxels (Fig. 5). The peaks of these clusters also survived small-volume correction (Table 1; peak SVC $p<0.05$).

ApEn in Familial AD Subjects

In Exp 2, ApEn was similarly calculated for 22 subjects from fAD families. Mean ApEn of gray matter showed a significant positive correlation with MMSE scores (Spearman $R=0.482$, $p=0.023$). This correlation between mean ApEn in gray matter and MMSE scores was still significant when multiple regression analysis was applied with age and mutation status included as covariates ($p=0.024$). Mean ApEn of white matter, however, did not show such trends with MMSE or CDR scores. Mean ApEn of gray or white matter did not show significant correlations with head motion parameters (maximum translation displacements and rotation angles) across the 22 subjects.

Voxel-wise regression of ApEn with MMSE or CDR-SOB scores was performed using GLM in SPM8, with age and mutation status included as covariates. Significant positive correlations between ApEn and MMSE scores were seen in the following regions: bilateral precuneus (PrC), right supramarginal gryus (SMG), right angular gryus (AG), left postcentral gyrus (PCG), right paracentral gyrus (PaCG), right superior temporal gyrus (STG), left lingual gyrus (LG), and right putamen (Put) (Fig. 6A, $p=0.001$, uncorrected). All of these clusters except the left precuneus survived small volume correction using corresponding ROIs defined in AAL (Table 2, peak SVC $p<0.05$). No significant negative correlation between ApEn and MMSE was observed. For CDR-SOB scores, significant negative correlations with ApEn were observed similarly in right precuneus (PrC), right supramarginal gryus (SMG), right angular gyrus (AG), left postcentral gyrus (PCG), and right paracentral gyrus (PaCG) (Fig. 6B, $p=0.001$, uncorrected), all of which survived small volume correction (Table 2, peak SVC $p<0.05$). No significant positive correlation between ApEn and CDR-SOB was observed. Significant clusters and peak voxels with peak SVC p values are listed in Table 2. Regression analysis of ApEn with age and mutation status showed that mutation in APP or PSEN1 genes was associated with decreased ApEn in the left parietal lobe ($p=0.001$, uncorrected; kc=10; peak SVC $p=0.035$). However, after including MMSE or CDR-SOB scores as covariates, no significant correlation between mutation status and ApEn was found. This result suggests that no significant mutation effect, independent of the effect of cognitive decline, is present.

Cross-Approximate Entropy

In Exp 1, voxel-wise C-ApEn was calculated using a single seed-voxel in the left precuneus, the peak of DMN based on meta-analysis. A smaller m=1 was used for the calculation of C-ApEn compared to m=2 for ApEn as suggested by literature (since the count of matched patterns between two time series would be too few for m=2)(6,10,25). The results demonstrated high synchronicity (lower C-ApEn) in some nodes of the DMN such as the precuneus/posterior cingulate cortex, and the medial prefrontal areas, as well as the gray matter in general. Average C-ApEn images of combined young and elderly subjects are displayed in Fig. 7. Voxel-by-voxel comparison showed a significant inverse relationship between C-ApEn and cross-correlation ($r=-0.473$, $N=1110$, $p<0.0001$) (Fig. 7, scatter plot). Interestingly, the anti-correlation between C-ApEn and cross-correlation was stronger in the young group ($r=-0.510$, $p<0.0001$) than that of the aged group ($r=-0.158$, $p<0.0001$).

DISCUSSION

Resting state BOLD fMRI time-series are generally considered to consist of three components: spontaneous fluctuations with metabolic and neuronal origin, physiological noise related to cardiac/respiratory pulsations, and scanner related thermal noise (16). A consensus has emerged from recent studies that temporal fluctuations in resting state BOLD fMRI, in particular low frequency components (<0.1Hz), arise primarily from spontaneous fluctuations of brain metabolism and neuronal activity (17,28). It has been demonstrated by Logothetis et al (29) that hemodynamic responses in BOLD signal correlate best with local field potentials (LFT) that are thought to reflect the weighted average of input signals on the dendrites and cell bodies of local neurons. Since there are approximately 200,000 dendrites on each neuron, neurons and glial cells form a highly complex and interconnected network that is controlled and balanced through myriad of feedback loops, even during resting state. Therefore, the complexity of resting state BOLD time-series may provide a viable measure to probe the complexity of the underlying brain activity.

The present study attempted to quantify the complexity of resting state BOLD fMRI using ApEn, which showed age-related decreases in healthy volunteers. It has been suggested that normal human aging is associated with a loss of complexity in a variety of fractal-like anatomic structures and physiological processes (1,2). Using a variety of measures that employ fractal analysis, aging has been shown to be associated with a loss of complexity in blood pressure, respiratory cycle, stride interval, and postural sway dynamics (9,30,31). It has been reported that aging may affect cortical and sub-cortical connections through cell loss, synaptic degeneration, blood flow reduction, neurochemical alteration as well as central nervous system reorganization (32). All these age-related changes may lead to gradual loss of both local and long-range connections in the brain, thereby decreasing complexity of spontaneous brain activity. The age related decline in ApEn of resting state fMRI BOLD time-series, observed in the present study, is therefore consistent with past findings. In particular, it has been reported that functional connectivity in the DMN reduces with normal aging (33), and further reduces in Alzheimer's disease patients, and persons at risk for dementia such as APOE-ε4+ carriers (34,35). The observed ApEn decreases with aging in bilateral angular gyri, right mid temporal gyrus, left supramarginal gyrus, left mid and posterior cingulate cortex (at the TE of 35ms) partially overlap with the DMN, suggesting potential associations between reduced functional connectivity and reduced ApEn or complexity of resting state BOLD fMRI with aging.

Another interesting finding from the present study is that ApEn is lowest at the TE of 35ms and shows significant differences between the 3 tissue types of the brain. Past studies have shown that the magnitude of spontaneous fluctuations of BOLD fMRI is TE dependent and displays a spatial distribution that is specific to neuroanatomical structures (16,17). For

instance, spontaneous fluctuations in BOLD fMRI demonstrate a stereotypical TE dependence with the magnitude reaching its peak when TE approximates T2*. The magnitude of spontaneous fluctuations in BOLD fMRI is higher in gray matter than that in white matter. The observed trend of ApEn variations with TE and tissue types in the present study was in general opposite of those of spontaneous fluctuations in BOLD fMRI. One potential explanation may be related to the fractional contributions of thermal and physiological noise to temporal fluctuations of BOLD fMRI. Since thermal or white noise yields the highest ApEn in all temporal processes, higher magnitude of physiological noise (i.e., lower fraction of thermal noise) may lead to lower ApEn values of BOLD fMRI with TE close to T2*. Similarly, higher ApEn in white matter may be attributed to a greater fraction of white noise in temporal fluctuations of white matter than that of gray matter, while pulsatile CSF movement may contribute to a low ApEn in CSF. This hypothesis, nevertheless, cannot fully account for our findings since the lowest ApEn was observed at the TE of 35ms instead of the predicted 50ms (closest to T2*). The biophysical mechanisms of observed TE and tissue type dependences of ApEn remain to be clarified in further experiments.

Compared to normal aging, neurodegenerative diseases might be expected to further reduce the complexity of brain activity, possibly affecting some brain structures more than others. In the present study, ApEn measurements were also performed on 22 subjects from families with fully-penetrant autosomal dominant AD. Cognitive impairment, as indicated by lower MMSE and higher CDR-SOB scores, was associated with lower mean ApEn in gray matter as well as reduced regional ApEn in the precuneus, right lateral parietal regions (i.e. supramarginal and angular gyri), and bilateral superior parietal regions (i.e. left postcentral and right paracentral gyri) (Fig. 6 and Table 2). Past morphometric MRI examinations in fAD revealed that the onset of dementia is accompanied by progressive medial temporal lobe and whole brain atrophy (36). FDG-PET studies of fAD subjects showed hypometabolism in temporoparietal, posterior cingulate/precuneus, and frontal cortical regions (37). SPECT perfusion imaging studies showed hypoperfusion in the hippocampal-amygdaloid complex and the anterior and posterior cingulate cortex (38). The detected pattern of ApEn decreases associated with cognitive decline is generally consistent with past metabolic and perfusion imaging studies in fAD.

Functional connectivity based on temporal correlations of resting state BOLD fMRI time-series is commonly used to characterize networks of the brain. It has been suggested that C-ApEn may provide a novel measure, complementary to cross-correlation and cross-spectrum analyses of two time series, while ApEn can be compared to their single variable counterparts, auto-correlation function and power spectrum (39). The advantage of C-ApEn and ApEn is that these nonlinear measurements do not require the assumptions for linear systems. However, the drawback is that C-ApEn and ApEn generally require longer time series compared to the calculation of their linear counterparts. C-ApEn may also be applied to derive indices to characterize the complexity of neural networks (40). The present study demonstrated a general anti-correlation between the asynchrony pattern of BOLD time series using C-ApEn and functional connectivity using cross-correlation, and this anti-correlation appeared to be stronger in young subjects compared to elderly subjects. Nevertheless, there are considerable differences between C-ApEn and cross-correlation analyses, e.g., the observed anti-correlation between C-ApEn and cross-correlation may represent the inverse relationship of these two measures in GM and WM. This issue awaits verification in future studies with increased number of acquisitions during BOLD fMRI scans.

The present study has several limitations. The sample size is relatively small and the number of BOLD acquisitions is not high (N=140 for Exp 2), which may affect the reliability of

ApEn measurements. Nevertheless, significant ApEn variations associated with normal aging and cognitive deterioration were detected within the relatively small cohort of subjects. The value of ApEn may not be directly interpreted as the degree of complexity, since random noise yields the highest ApEn but does not represent the most complex process. Improved complexity measures such as multi-scale ApEn and Sample Entropy (SampEn) may be applied to address this in future studies (5,25). The use of small volume correction in pixel-wise correlation analyses without a priori hypothesis may be biased. Since the goal of the present study was to introduce and explore ApEn as a novel measure of complexity or regularity of resting-state BOLD fMRI, it is beyond the scope of this work to fully investigate the effects of aging, genetic factors and dementia using ApEn. The clinical value of ApEn and C-ApEn awaits a full evaluation in future studies using large data sets.

In conclusion, the present study explored ApEn as a measure of complexity or regularity of resting state BOLD fMRI series. The results showed that ApEn decreases with normal aging and cognitive decline in fAD subjects. Cross-ApEn was further applied to measure the asynchrony of BOLD fMRI series between voxels. ApEn and C-ApEn may offer novel nonlinear approaches for assessing the complexity and synchronicity of brain activity in normal aging and cognitive decline associated with neurodegenerative diseases.

Acknowledgments

Grant Support: NIH R01-MH080892, P50-AG016570, U01-AG032438, the Easton Consortium for Alzheimer's Disease Drug and Biomarker Discovery

REFERENCES

1. Lipsitz LA. Physiological complexity, aging, and the path to frailty. Science of aging knowledge environment: SAGE KE. 2004; 2004:pe16. [PubMed: 15103055]
2. Goldberger AL. Non-linear dynamics for clinicians: chaos theory, fractals, and complexity at the bedside. The Lancet. 1996; 347:1312–1314.
3. Mandelbrot, B. The Fractal Geometry of Nature. First Edition. W. H. Freeman; 1982. p. 460
4. Goldberger AL, West BJ. Fractals in physiology and medicine. The Yale Journal of Biology and Medicine. 1987; 60:421–435. [PubMed: 3424875]
5. Costa M, Goldberger A, Peng C-K. Multiscale entropy analysis of complex physiologic time series. Physical Review Letters. 2002; 89:068102.1–068102.4. [PubMed: 12190613]
6. Pincus SM. Approximate entropy as a measure of system complexity. Proceedings of the National Academy of Sciences of the United States of America. 1991; 88:2297–2301. [PubMed: 11607165]
7. Schuckers SAC, Raphisak P. Distinction of arrhythmias with the use of approximate entropy. Computers in Cardiology. 1999; i:347–350.
8. Ryan SM, Goldberger AL, Pincus SM, Mietus J, Lipsitz LA. Gender- and age-related differences in heart rate dynamics: are women more complex than men? Journal of the American College of Cardiology. 1994; 24:1700–1707. [PubMed: 7963118]
9. Kaplan DT, Furman MI, Pincus SM, Ryan SM, Lipsitz LA, Goldberger AL. Aging and the complexity of cardiovascular dynamics. Biophysical Journal. 1991; 59:945–949. [PubMed: 2065195]
10. Pincus SM. Approximate entropy as a measure of irregularity for psychiatric serial metrics. Bipolar Disorders. 2006; 8:430–440. [PubMed: 17042881]
11. Abásolo D, Hornero R, Espino P, Poza J, Sánchez CI, de la Rosa R. Analysis of regularity in the EEG background activity of Alzheimer's disease patients with Approximate Entropy. Clinical Neurophysiology. 2005; 116:1826–1834. [PubMed: 15979403]
12. Pincus SM, Keefe DL. Quantification of hormone pulsatility via an approximate entropy algorithm. American Journal of Physiology. 1992:E741–E754. [PubMed: 1590385]
13. Zarahn E, Aguirre GK, D'Esposito M. Empirical analyses of BOLD fMRI statistics. NeuroImage. 1997; 5:179–197. [PubMed: 9345548]

14. Wang J, Aguirre GK, Kimberg DY, Roc AC, Li L, Detre JA. Arterial spin labeling perfusion fMRI with very low task frequency. Magnetic Resonance in Medicine. 2003; 49:796–802. [PubMed: 12704760]
15. Bullmore E, Fadili J, Maxim V, Sendur L, Whitcher B, Suckling J, et al. Wavelets and functional magnetic resonance imaging of the human brain. NeuroImage. 2004; 23:S234–S249. [PubMed: 15501094]
16. Krüger G, Glover GH. Physiological noise in oxygenation-sensitive magnetic resonance imaging. Magnetic Resonance in Medicine. 2001; 46:631–637. [PubMed: 11590638]
17. Yan L, Zhuo Y, Ye Y, Xie SX, An J, Aguirre GK, et al. Physiological origin of low-frequency drift in blood oxygen level dependent (BOLD) functional magnetic resonance imaging (fMRI). Magnetic Resonance in Medicine. 2009; 61:819–827. [PubMed: 19189286]
18. Biswal BB, Mennes M, Zuo X-N, Gohel S, Kelly C, Smith SM, et al. Toward discovery science of human brain function. Proceedings of the National Academy of Sciences of the United States of America. 2010; 107:4734–4739. [PubMed: 20176931]
19. Zang Y-F, He Y, Zhu C-Z, Cao Q-J, Sui M-Q, Liang M, et al. Altered baseline brain activity in children with ADHD revealed by resting-state functional MRI. Brain and Development. 2007; 29:83–91. [PubMed: 16919409]
20. Sokunbi MO, Staff RT, Waiter GD, Ahearn TS, Fox HC, Deary IJ, et al. Inter-individual differences in fMRI entropy measurements in old age. IEEE Transactions on Biomedical Engineering. 2011; 58:3206–3214. [PubMed: 21859598]
21. Chang C, Glover GH. Time-frequency dynamics of resting-state brain connectivity measured with fMRI. NeuroImage. 2010; 50:81–98. [PubMed: 20006716]
22. Folstein MF, Folstein SE, McHugh PR. “Mini-mental state”. A practical method for grading the cognitive state of patients for the clinician. Journal of psychiatric research. 1975; 12:189–198. [PubMed: 1202204]
23. Morris JC. Clinical dementia rating: a reliable and valid diagnostic and staging measure for dementia of the Alzheimer type. International Psychogeriatrics. 1997; S1:173–178. [PubMed: 9447441]
24. Yan L, Zhuo Y, Wang B, Wang DJJ. Loss of Coherence of Low Frequency Fluctuations of BOLD FMRI in Visual Cortex of Healthy Aged Subjects. The Open Neuroimaging Journal. 2011; 5:105–111. [PubMed: 22216081]
25. Richman JS, Moorman JR. Physiological time-series analysis using approximate entropy and sample entropy. American Journal of Physiology. 2000; 278:H2039–H2049. [PubMed: 10843903]
26. Toro R, Fox PT, Paus T. Functional coactivation map of the human brain. Cerebral Cortex. 2008; 18:2553–2559. [PubMed: 18296434]
27. Chao-Gan Y, Yu-Feng Z. DPARSF: A MATLAB Toolbox for “Pipeline” Data Analysis of Resting-State fMRI. Frontiers in Systems Neuroscience. 2010; 4:13.1–13.7. [PubMed: 20577591]
28. Fox MD, Raichle ME. Spontaneous fluctuations in brain activity observed with functional magnetic resonance imaging. Nature Neuroscience. 2007; 8:700–711.
29. Logothetis NK, Pauls J, Augath M, Trinath T, Oeltermann A. Neurophysiological investigation of the basis of the fMRI signal. Nature. 2001; 412:150–157. [PubMed: 11449264]
30. Hausdorff JM, Mitchell SL, Firtion R, Peng CK, Cudkowicz ME, Wei JY, et al. Altered fractal dynamics of gait: reduced stride-interval correlations with aging and Huntington’s disease. Journal of Applied Physiology. 1997; 82:262–269. [PubMed: 9029225]
31. Peng CK, Mietus JE, Liu Y, Lee C, Hausdorff JM, Stanley HE, et al. Quantifying fractal dynamics of human respiration: age and gender effects. Annals of Biomedical Engineering. 2002; 30:683–692. [PubMed: 12108842]
32. Craik FIM, Salthouse TA. The Handbook of Aging and Cognition. 2000:755.
33. Damoiseaux JS, Beckmann CF, Arigita EJS, Barkhof F, Scheltens P, Stam CJ, et al. Reduced resting-state brain activity in the “default network” in normal aging. Cerebral Cortex. 2008; 18:1856–1864. [PubMed: 18063564]
34. Greicius MD, Srivastava G, Reiss AL, Menon V. Default-mode network activity distinguishes Alzheimer’s disease from healthy aging: evidence from functional MRI. Proceedings of the

National Academy of Sciences of the United States of America. 2004; 101:4637–4642. [PubMed: 15070770]

35. Sheline YI, Morris JC, Snyder AZ, Price JL, Yan Z, D'Angelo G, et al. APOE4 allele disrupts resting state fMRI connectivity in the absence of amyloid plaques or decreased CSF A 42. The Journal of Neuroscience. 2010; 30:17035–17040. [PubMed: 21159973]
36. Fox NC, Crum WR, Scahill RI, Stevens JM, Janssen JC, Rossor MN. Imaging of onset and progression of Alzheimer's disease with voxel-compression mapping of serial magnetic resonance images. Lancet. 2001 Jul.358:201–205. [PubMed: 11476837]
37. Kennedy AM, Frackowiak RS, Newman SK, Bloomfield PM, Seaward J, Roques P, et al. Deficits in cerebral glucose metabolism demonstrated by positron emission tomography in individuals at risk of familial Alzheimer's disease. Neuroscience Letters. 1995; 186:17–20. [PubMed: 7783942]
38. Johnson KA, Albert MS. Perfusion abnormalities in prodromal AD. Neurobiology of Aging. 2000; 21:289–292. [PubMed: 10867213]
39. Pincus SM. Older males secrete luteinizing hormone and testosterone more irregularly, and jointly more asynchronously, than younger males. Proceedings of the National Academy of Sciences of the United States of America. 1996; 93:14100–14105. [PubMed: 8943067]
40. Tononi G, Sporns O, Edelman GM. A measure for brain complexity: relating functional segregation and integration in the nervous system. Proceedings of the National Academy of Sciences of the United States of America. 1994; 91:5033–5037. [PubMed: 8197179]

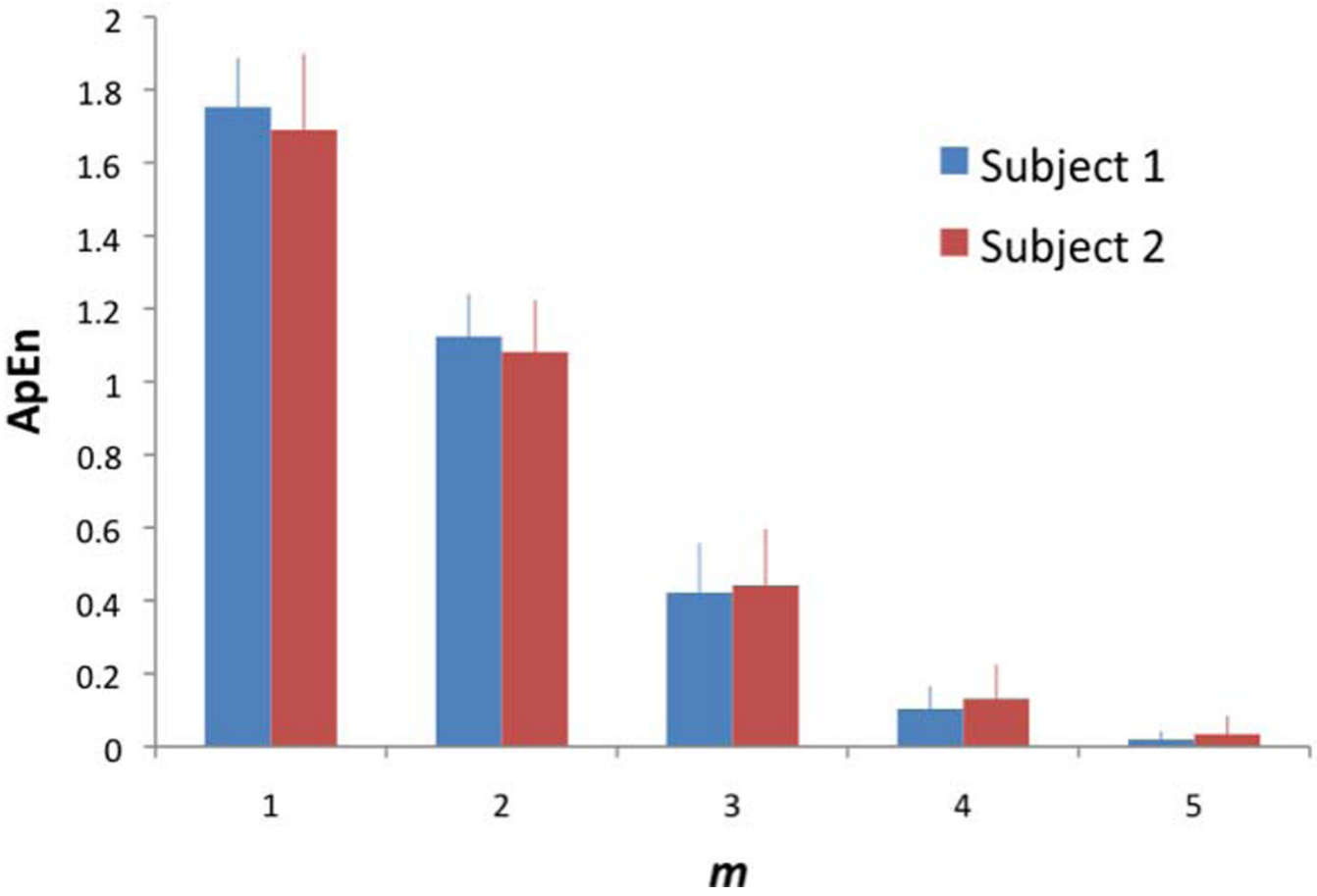

Figure 1.
Effect of sliding window width (*m*) on ApEn in 2 representative subjects (r=0.25 × SD, N=240). Error bars indicate SD.

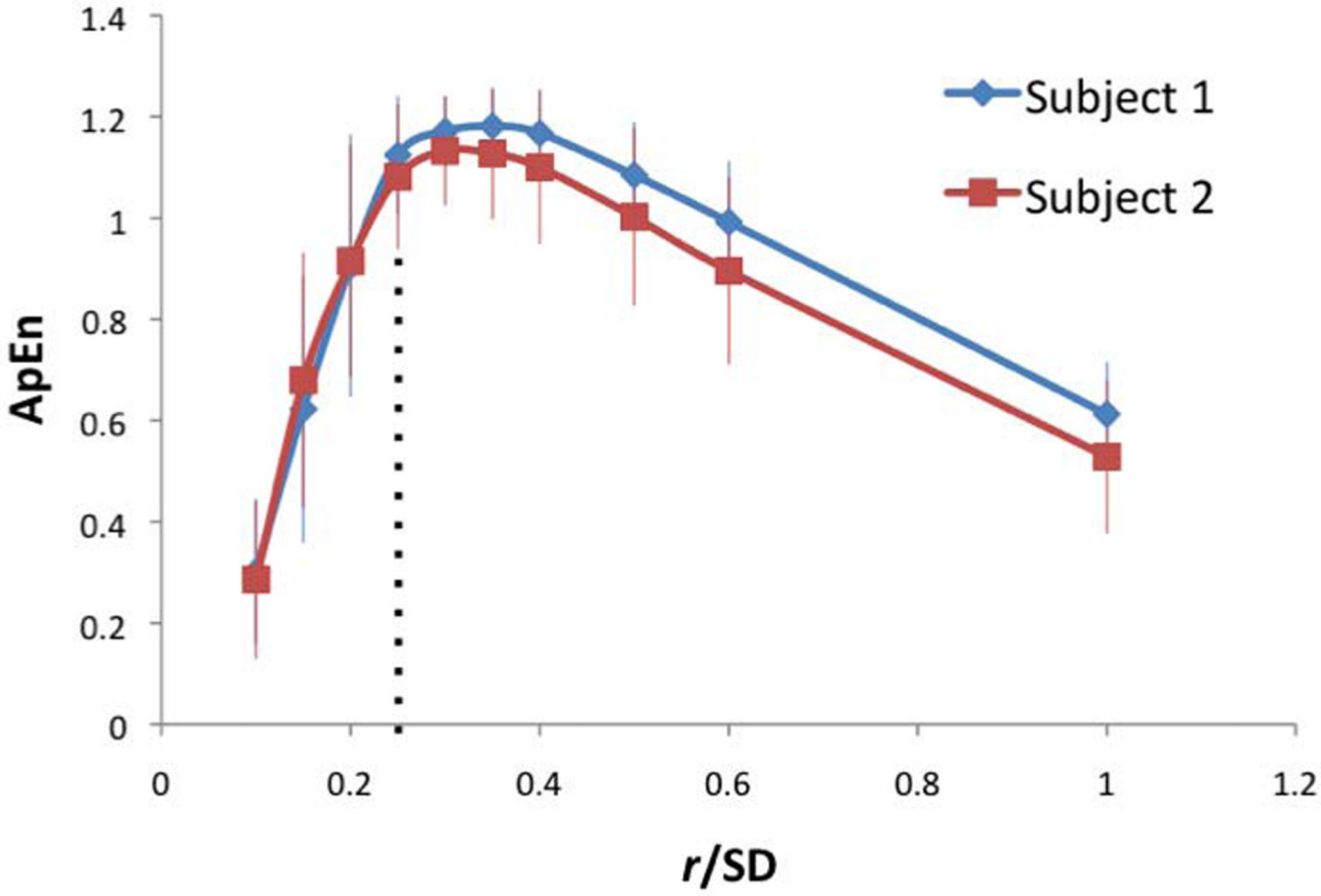

Figure 2.
Effect of tolerance width (*r*) on ApEn in 2 representative subjects (*m*=2, N=240). Error bars indicate SD. Dotted-line indicates r=0.25 × SD.

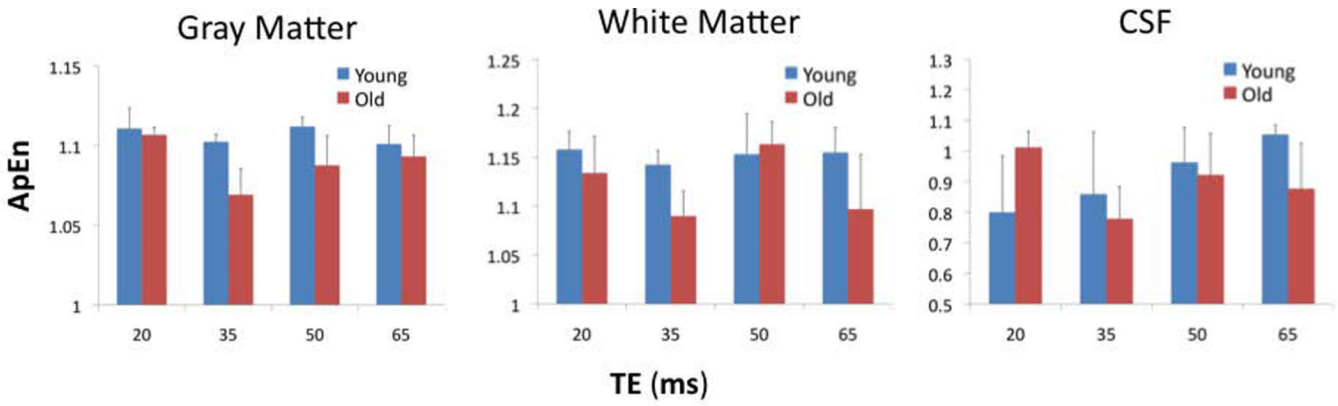

Figure 3.
Bar chart of mean ApEn of gray matter, white matter, and cerebral spinal fluid in the 2 age groups across 4 TEs. Error bars indicate SD.

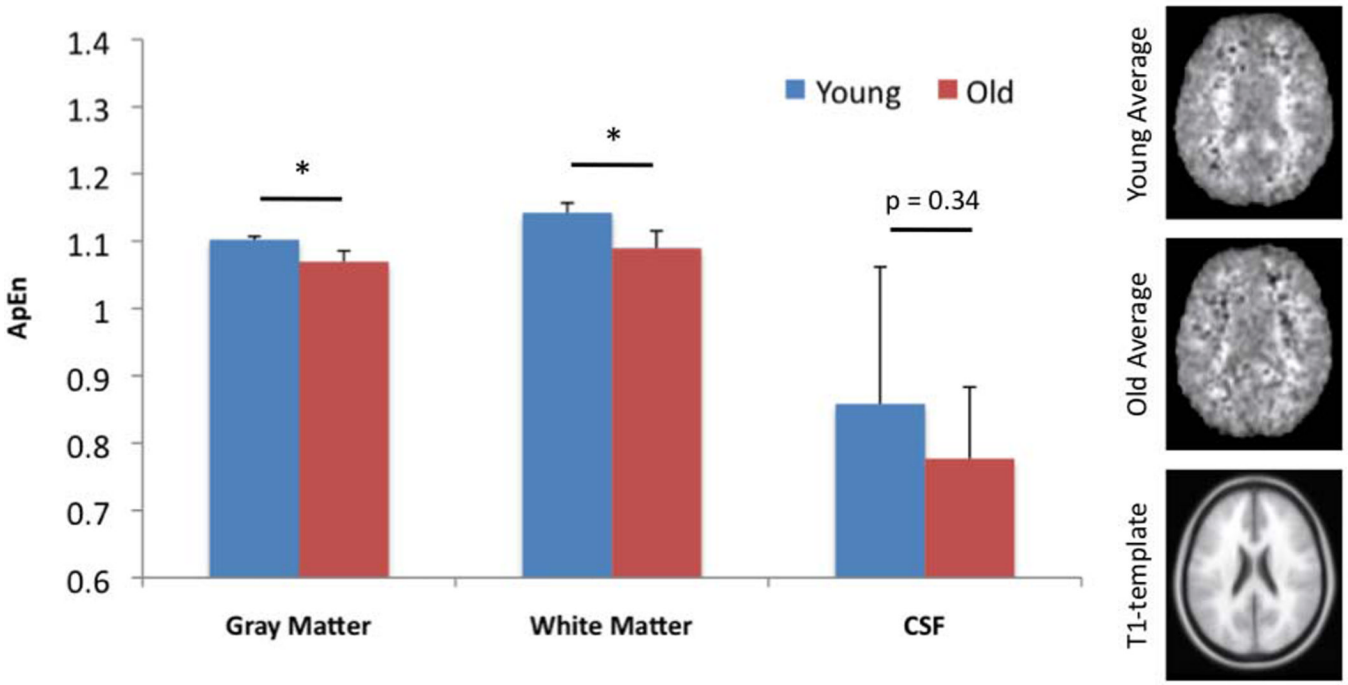

Figure 4.
Mean ApEn values and maps acquired at the representative TE of 35ms in the 2 age groups. Error bars indicate SD. Significant differences are seen between young and old in gray and white matter (*, $p \leq 0.002$).

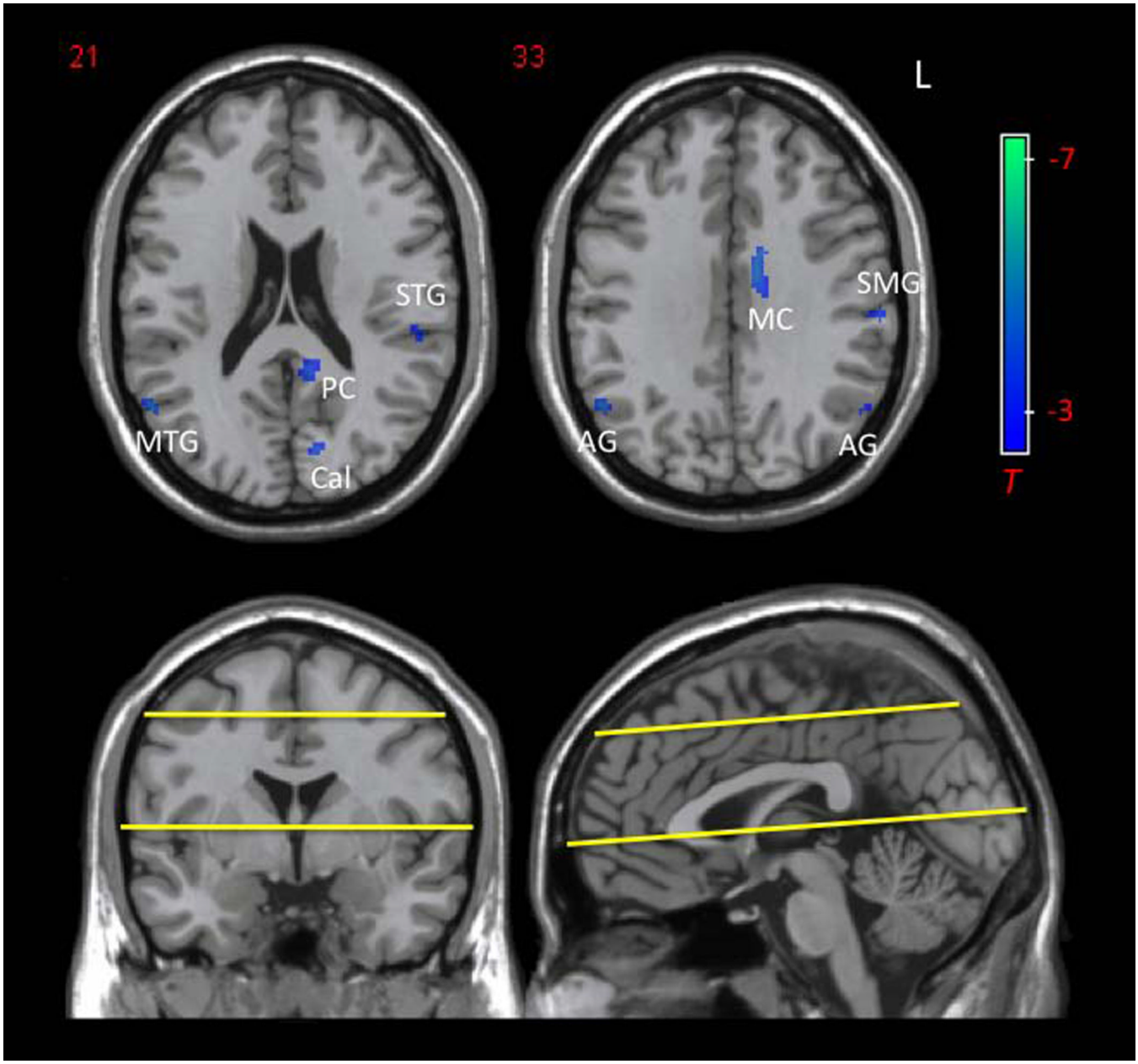

Figure 5.

Reduced regional ApEn in aged compared to young subjects. Significant ApEn reduction is found in bilateral angular gyri (AG), right mid temporal gyrus (MTG), left supramarginal gyrus (SMG), left mid and posterior cingulate cortex (MC and PC), and left calcarine cortex (Cal) (uncorrected p=0.001, T=3.8, kc=10; peak SVC p<0.05). Yellow lines indicate the upper and lower limits of brain volume examined (10 slices).

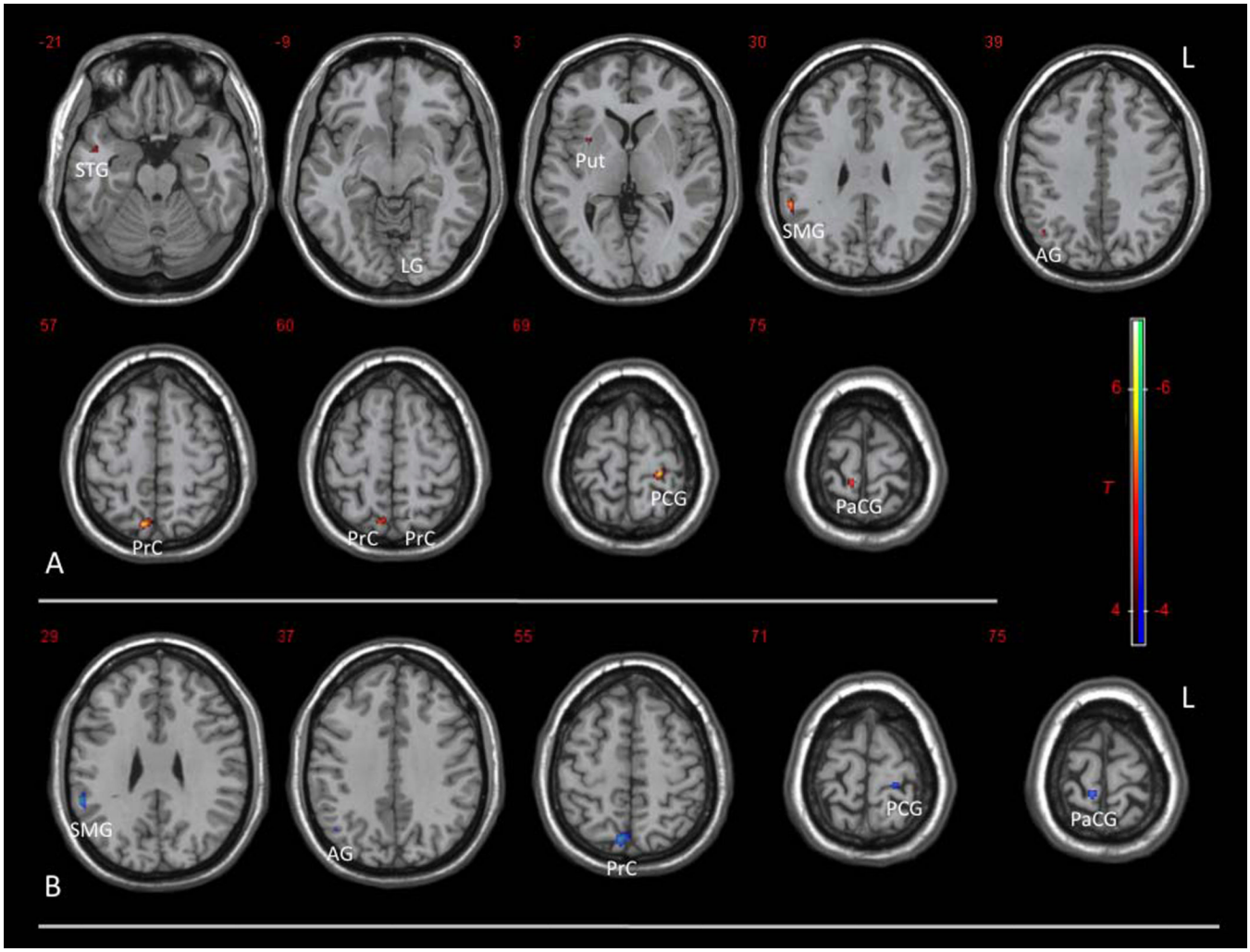

Figure 6.

Voxel-wise correlations of ApEn with (A) Mini-Mental Status Exam (MMSE) and (B) Clinical Dementia Rating Sum of Box (CDR-SOB) scores. Significant correlations between ApEn and MMSE or CDR-SOB scores are observed in these regions: bilateral precuneus (PrC), right supramarginal gryus (SMG), right angular gryus (AG), left postcentral gyrus (PCG), right paracentral gyrus (PaCG), right superior temporal gyrus (STG), left lingual gryus (LG), and right putamen (Put) (uncorrected p=0.001, T=3.9, kc=10; peak SVC p<0.05, except for left PrC).

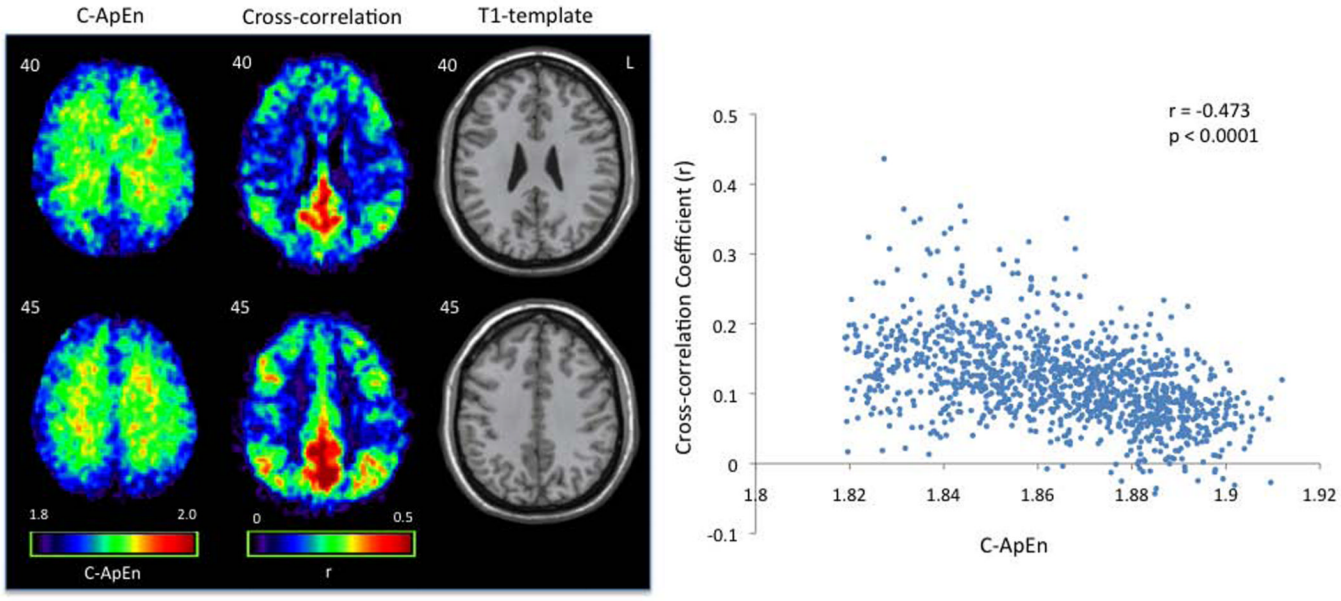

Figure 7.

Cross-approximate entropy (C-ApEn) and cross-correlation maps using a left precuneus seed demonstrate regional anti-correlation. Average C-ApEn and cross-correlation maps of the 16 healthy subjects (8 young and 8 old) are shown along with their T1 structural maps. A scatter plot of the average images on the right shows significant inverse relationship between C-ApEn and cross-correlation across brain pixels ($r=-0.473$, $N=1110$, $p<0.0001$).

Table 1

Reduced regional ApEn in aged compared to young subjects at TE=35ms

Brain Region	Cluster Centraid (x, y, z)	Cluster Size (k_c)	Peak T	Peak SVC p
Right Mid Temporal Gyrus and Angular Gyrus	52, −62, 24	149	8.02	0.001
Left Mid Cingulum	−12, −6, 34	86	5.98	0.007
Left Calcarine Cortex	−14, −78, 16	21	5.70	0.005
Left Supramarginal Gyrus	−62, −22, 32	27	4.78	0.012
Left Posterior Cingulum	−10, −46, 18	41	4.77	0.006
Left Superior Temporal Gyrus	−54, −30, 18	19	4.45	0.031
Left Angular Gyrus	−56, −62, 32	13	4.32	0.023

Level of significance is set at uncorrected p=0.001 (T=3.8), with $k_C \geq 10$. Peak p values after small volume correction using AAL ROIs are shown. All have peak SVC p<0.05.

Table 2

Clusters showing positive correlations between ApEn and MMSE, and negative correlations between ApEn and CDR

Brain Region	Cluster Centraid (x, y, z)	Cluster Size (k_c)	Peak T	Peak SVC p
MMSE Positive Correlation				
Left Postcentral Gyrus	−24,−32, 68	49	6.52	0.001
Right Precuneus	8, −70, 56	103	6.22	0.002
Right Supramarginal Gyrus	56,−42,30	52	5.85	0.002
Right Paracentral Lobule	8, −38, 72	38	5.50	0.002
Right Angular Gyrus	44, −62, 40	19	4.85	0.009
Right Mid Temporal Gyrus	46, 0, −20	27	4.44	0.044
Right Putamen	30, 6, 2	12	4.41	0.013
Left Lingual Gyrus	−14, −68, −12	19	4.36	0.027
Left Precuneus	−14, −64, 60	10	3.92	0.084$^{\otimes}$
CDR-SOB Negative Correlation				
Right Supramarginal Gyrus	56, −44, 28	57	6.61	0.001
Right Precuneus	6, −72, 54	164	6.08	0.002
Right Paracentral Lobule	8, −38, 74	28	5.27	0.002
Left Postcentral Gyrus	−22, −32, 70	33	5.11	0.008
Right Angular Gyrus	44, −64, 38	11	4.20	0.029

Age and mutation status are included in the regression analyses. Level of significance is set at uncorrected p=0.001 (T=3.9), with $k_C \geq 10$. Peak p values after small volume correction using AAL ROIs are shown. All except the left precuneus cluster ($^{\otimes}$) have peak SVC p<0.05